Plant, Cell and Environment (2016) 39, 233–244 doi: 10.1111/pce.12541

Original Article

Separating water-potential induced swelling and shrinking from measured radial stem variations reveals a cambial growth and osmotic concentration signal

Tommy Chan[1], Teemu Hölttä[1], Frank Berninger[1], Harri Mäkinen[2], Pekka Nöjd[2], Maurizio Mencuccini[3] & Eero Nikinmaa[1]

[1]Department of Forest Ecology, University of Helsinki, Helsinki FIN-00014, Finland, [2]Finnish Forest Research Institute, Vantaa FIN-01301, Finland and [3]School of GeoSciences, University of Edinburgh, Edinburgh EH9 3JN, UK

ABSTRACT

The quantification of cambial growth over short time periods has been hampered by problems to discern between growth and the swelling and shrinking of a tree stem. This paper presents a model, which separates cambial growth and reversible water-potential induced diurnal changes from simultaneously measured whole stem and xylem radial variations, from field-measured Scots pine trees in Finland. The modelled growth, which includes osmotic concentration changes, was compared with (direct) dendrometer measurements and microcore samples. In addition, the relationship of modelled growth and dendrometer measurements to environmental factors was analysed. The results showed that the water-potential induced changes of tree radius were successfully separated from stem growth. Daily growth predicted by the model exhibited a high correlation with the modelled daily changes of osmotic concentration in phloem, and a temperature dependency in early summer. Late-summer growth saw higher dependency on water availability and temperature. Evaluation of the model against dendrometer measurements showed that the latter masked a true environmental signal in stem growth due to water-potential induced changes. The model provides better understanding of radial growth physiology and offers potential to examine growth dynamics and changes due to osmotic concentration, and how the environment affects growth.

Key-words: dendrometer; elasticity; hydraulic conductance; phloem; xylem.

INTRODUCTION

Tree growth is probably the single most studied process in forest science, but we still do not fully understand its exact dependence upon environmental conditions, particularly at short-term timescales. The analysis of stem growth is hampered by the multiple factors influencing it (Deslauriers & Morin 2005). The environment directly influences not only the cambial processes (e.g. cell division and expansion) but also the photosynthetic production, carbohydrate allocation and water relations of a tree (Hölttä *et al*. 2010). These factors interact with hormonal control, influencing growth in a complex way (Altman & Goren 1974).

One common method to study intra-annual growth is based upon measured stem diameter or radial variations with dendrometers. However, the task of deriving stem growth from dendrometer measurements is more difficult than initially assumed. The variations of stem radius measured over bark are caused by two processes: irreversible cambial growth due to accumulation of new woody and bark tissue material and reversible changes (i.e. swelling and shrinking) that can be rapid (Daudet *et al*. 2005) or more gradual (Mencuccini *et al*. 2013). Much of the reversible change arise from sap movement from higher to lower water potential along the xylem tract and the exchange of water between the xylem and phloem tissues (Whitehead & Jarvis 1981). These changes can ultimately mask short-term growth and hamper our ability to use dendrometer measurements for assessing actual cambial growth. This is especially evident during drought periods, when the stem dehydrates and shrinks and then rehydrates after rainfall (Buell *et al*. 1961; Bordiert 1994). Thus, short-term, transpiration-driven changes must be separated from the longer term variations of stem dimensions to fully understand cambial growth and its interactions with tree physiology and responses to changing environmental factors. In addition to water-potential-driven, predominantly diurnal change, more gradual diameter changes also occur concomitantly as the osmotic concentration in the phloem – caused by changes in the soluble carbohydrate concentration – varies (Sevanto *et al*. 2003). Therefore, an increase in osmotic concentration will draw water from the roots and thus increase the stem diameter (Mencuccini *et al*. 2013). Measured stem diameter may also change gradually due to change in the moisture content of the bark (Gall *et al*. 2002).

Models have been used to relate changes in stem radius to xylem sap flow dynamics influenced by water uptake and transpiration (Zweifel & Häsler 2001; Zweifel *et al*. 2001). These approaches used a sap flow and storage methodology, where water potential is the driver for linking changes of stem diameter to water stored in the stem. More recent water storage and sap flow models have linked variations in stem radius to both water relations and cambial growth (Steppe *et al*. 2006; De Schepper & Steppe 2010; Hölttä *et al*. 2010)

Correspondence: T. Chan. e-mail: tommy.chan@helsinki.fi

and changes in phloem osmotic concentration (Mencuccini *et al*. 2013). These approaches offer new possibilities to study stem growth dynamics by separating the changes related to stem water status.

The purpose of this study was to use a model to separate the water-induced (i.e. water-potential induced) component of measured radial stem variations to reveal a proxy for stem growth and changes due to osmotic concentration. Secondly, we studied how environmental factors influenced these reversible and irreversible variations at a daily and intra-annual timescale. Finally, we compared the model predictions against measured tracheid formation from microcores and dendrometer data, whereby the latter included both reversible and irreversible components.

MATERIALS AND METHODS

Model to estimate long-term radial variations

A hydraulic model based upon the principles presented by Mencuccini *et al*. (2013) was used to separate the water-induced changes of the inner bark from other radial variations. The inner bark is defined here as the vascular cambium, the newly formed xylem and the phloem tissue produced to the outside of the pre-existing xylem tissue (Fig. 1). If the water-induced component of the inner-bark radius, which is related to changes in the xylem water potential, can be separated successfully, we can claim that its remaining increment can be used as a proxy for growth (which includes newly grown xylem and phloem tissue) and its changes due to osmotic concentration.

The model assumes that the xylem and inner bark exchange water along the water potential gradient in the radial direction (Hölttä *et al*. 2009). As xylem water potential and radial stem changes are closely related (see the Theory section), the model will require four inputs: inner-bark radius (D_b), xylem radius (D_x), xylem radial hydraulic conductance (α) and the ratio of the elastic properties of inner bark to xylem (β). Both α and β parameters affect daily radial stem variations (Sevanto *et al*. 2011) and need to be estimated from the measurements, whereas the radial inputs are measured from dendrometers. The dendrometers measured the whole stem radius (D_w) and D_x variations. The difference between these two dendrometer measurements is the inner-bark radius (D_b) (refer to Table 1 for terminology used in the study).

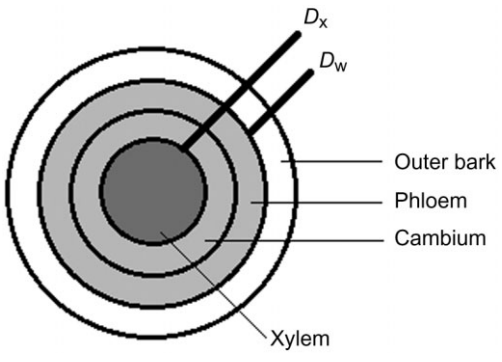

Figure 1. Cross section of a stem (N.B. not to scale). Two dendrometers (black bars) measured xylem (D_x) and whole stem (D_w) radius. To measure D_x, a dendrometer head rested on a screw inserted 10 mm through the outer and inner bark into the xylem. To measure D_w (light grey shade), the outer bark was removed and the head of the second dendrometer was placed on the phloem. The difference between D_w and D_x is the inner bark (D_b) (dark grey shade), which includes the vascular cambium and newly formed xylem and phloem tissue.

Table 1. A summary of the terminology and definitions used in the current study

Terminology	Definition
Increment	Irreversible quantitative radial increase due to new wood formation
Change	Reversible swelling and shrinking
Variation	Increment and/or change
D_w	Whole stem radial thickness
D_b	Inner-bark radial thickness
D_x	Xylem radial thickness
$\hat{\Delta}D_b$	Inner-bark radial change due solely to movement of water between the xylem and inner bark
$\hat{\Delta}G_m$	Modelled radial cambial growth and change of radius due to osmotic concentration movement
α	Parameter related to the radial hydraulic conductance between the xylem and inner-bark (see Eqn. 7)
β	The ratio of the diurnal amplitudes of D_b and D_x when xylem and inner-bark pressure changes are identical
P_0	Reversible peak in $\hat{\Delta}G_m$ due to changes in osmotic concentration
g	Linear-derived estimate of daily growth from $\hat{\Delta}G_m$

The model separates the variations of the inner bark into two distinct components. The first component ($\hat{\Delta}D_b$) is solely due to the movement of water between the xylem and inner bark, driven by changes in the xylem water potential (Fig. 2). We define the quantity of the second component as $\hat{\Delta}G_m = \Delta D_b - \hat{\Delta}D_b$, which is obtained as the residual after $\hat{\Delta}D_b$ has been subtracted from the measured inner-bark radius. $\hat{\Delta}G_m$ is therefore defined as all other processes influencing dimensional variations of the inner bark (i.e. due to cambial growth and changes in the inner-bark osmotic concentration).

Theory

Changes in xylem diameter reflect changes in xylem water pressure (ΔP_x) according to Hooke's law (Perämäki *et al*. 2001):

$$\frac{dD_x}{\Delta t} = \frac{d_{x,0}}{E_{r,x}} \frac{\Delta P_x}{\Delta t}, \quad (1)$$

where $d_{x,0}$ is the xylem diameter at a reference pressure, $E_{r,x}$ is the radial elastic modulus of the xylem tissue, Δt is the change in time and dD_x refers to the corresponding xylem

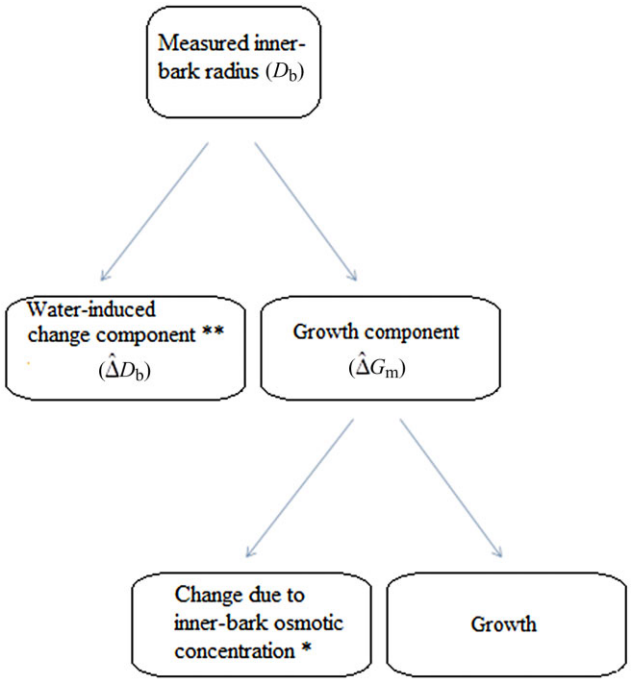

Figure 2. Schematic diagram of the partitioning of inner-bark (D_b) radius variation. D_b includes variation due to a cambial growth increment component ($\hat{\Delta}G_m$) and water-induced change component ($\hat{\Delta}D_b$). The current model separated the water-induced change component from D_b to reveal $\hat{\Delta}G_m$, which includes growth and change due to inner-bark osmotic concentration movement. The asterisks denote key differences in diurnal and seasonal amplitudes of stem radius variations, respectively.

diameter change over time (i.e. subsequent intervals). The xylem sap is assumed to be pure water, and hence, the water potential and pressure are equal. The same can be written for the changes in the inner-bark diameter, dD_b:

$$\frac{dD_b}{\Delta t} = \frac{d_{b,0}}{E_{r,b}} \frac{\Delta P_b}{\Delta t}, \tag{2}$$

where ΔP_b is the change in the 'average' turgor pressure of the inner bark, $d_{b,0}$ is the inner-bark diameter at a reference pressure and $E_{r,b}$ is the radial elastic modulus of the inner bark. The inner bark tends towards water potential equilibrium with the xylem by exchanging water with the xylem, when in disequilibrium. Water flux J ($m^3\ s^{-1}$) between the xylem and inner bark is

$$J = LA[P_x - (P_b - \Pi)], \tag{3}$$

where L is the area-specific radial hydraulic conductance between xylem and inner bark, A is the area through which water exchange takes place (assumed to be the area of the inner bark) and Π is the osmotic pressure of the inner bark.

Model for osmotic concentration change and growth

The rate of change in the pressure of the inner bark due to water movement induced by the water potential difference between the xylem and inner bark is as follows (from Eqns 2 and 3):

$$\frac{\Delta P_b}{\Delta t} = \frac{E_{r,b} J}{V_{b,0}} = \frac{E_{r,b}}{V_{b,0}} LA[P_x - (P_b - \Pi)], \tag{4}$$

where $V_{b,0}$ is the inner-bark volume at a reference pressure. Equation 4 can be rephrased so that the pressure terms are expressed in relation to the reference values (subscript 'ref'), for example, values at the beginning of the period under study:

$$\frac{\Delta P_b}{\Delta t} = \frac{E_{r,b}}{V_{b,0}} LA[(P_x - P_{x,ref}) - (P_b - P_{b,ref}) + (\Pi - \Pi_{ref})] - \frac{\Delta P_{b,ref}}{\Delta t}. \tag{5}$$

As we assume that at this point the osmotic concentration of the inner bark is constant (i.e. does not change with time), we can substitute Π with its reference value Π_{ref} so that the last term on the right-hand side vanishes. Writing $\Delta P_x = P_x - P_{x,ref}$ and $\Delta P_b = P_b - P_{b,ref}$ (and using Eqns 1 and 2):

$$\frac{\Delta P_b}{\Delta t} = \frac{E_{r,b}}{V_{b,0}} LA\left(\frac{E_{r,x}}{d_{x,0}} \Delta D_x - \frac{E_{r,b}}{d_{b,0}} \Delta D_b\right) - \frac{\Delta P_{b,ref}}{\Delta t}, \tag{6}$$

where ΔD_x and ΔD_b are the measured changes in xylem and inner-bark diameters, respectively, relative to a reference state (i.e. at the beginning of the measurement period). The quantities ΔD_x and ΔD_b are defined as $\Delta D_x = dD_x - d_{x,0}$ and $\Delta D_b = dD_b - d_{b,0}$, respectively.

The time derivate of the inner-bark diameter variation can further be expressed in terms of the diameters of the xylem and inner bark:

$$\begin{aligned} \frac{dD_b}{\Delta t} &= \frac{d_{b,0}}{E_{r,b}} \frac{\Delta P_b}{\Delta t} = \frac{d_{b,0} E_{r,b}}{E_{r,b} V_{b,0}} LA\left(\frac{E_{r,x}}{d_{x,0}} \Delta D_x - \frac{E_{r,b}}{d_{b,0}} \Delta D_b\right) - \frac{\Delta P_{b,ref}}{\Delta t} \\ &= \frac{LA}{V_{b,0}} E_{r,b}\left(\frac{d_{b,0} E_{r,x}}{d_{x,0} E_{r,b}} \Delta D_x - \Delta D_b\right) - \frac{\Delta P_{b,ref}}{\Delta t} \\ &= \alpha(\beta \Delta D_x - \Delta D_b) - \gamma, \end{aligned} \tag{7}$$

where α is the xylem radial hydraulic conductance between the xylem and inner bark, β is the ratio of the elastic properties of the inner bark to xylem for a given change in xylem water potential and $\gamma = \Delta P_{b,ref}/\Delta t$ is a constant equal to the rate of change of inner-bark pressure at the reference time.

Similarly to Mencuccini *et al.* (2013), the inner-bark diameter (affected only by xylem water potential) at time $(t + \Delta t)$ (i.e. the next measuring point) can be predicted from the changes in the inner-bark and xylem diameters at time (t):

$$\hat{\Delta} D_b(t + \Delta t) = \hat{\Delta} D_b(t) + \alpha\left[\beta \Delta D_x(t) - \hat{\Delta} D_b(t)\right] \Delta t, \tag{8}$$

where the caret is used to denote the predicted change for the inner-bark diameter solely due to changes in xylem water

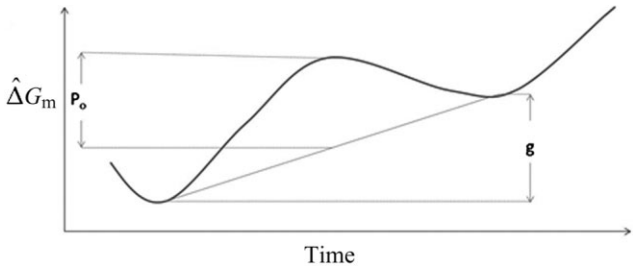

Figure 3. Schematic presentation of calculating the variation in daily estimated growth (g) and osmotic pressure (concentration) (P_0). The continuous black line is the estimated growth component that includes both P_0 and g. g includes the newly grown xylem and phloem tissue and is estimated as the difference of two consecutive minimum values of $\hat{\Delta}G_m$. The osmotic pressure is calculated from the daily amplitude of $\hat{\Delta}G_m$, by subtracting the interpolated growth (g) at the timing of the peak value of $\hat{\Delta}G_m$ from the peak value. For simplicity, a linear interpolation between the consecutive minimum values was used for g. However, its value at the peak of $\hat{\Delta}G_m$ would not have been much different even if a more complex interpolation was used that considers the changes in growth rate between day and night.

potential, and as in Mencuccini *et al.* (2013), the term γ has been omitted as it is only relevant for the first time point after the start of the measurements.

As defined previously, the difference between the measured inner-bark diameter (ΔD_b) and inner-bark diameter predicted from xylem water potential alone ($\hat{\Delta}D_b$) reveals the variation in the inner-bark diameter that is not explained by the xylem water potential ($\hat{\Delta}G_m$), which was used as a proxy for radial growth and changes due to osmotic concentration in this study:

$$\hat{\Delta}G_m(t) = \Delta D_b(t) - \hat{\Delta}D_b(t). \quad (9)$$

For the current study, we do not attempt to further separate the $\hat{\Delta}G_m$ signal into an osmotic concentration signal and growth signal. However, we make a simple estimation how they may be correlated (see the Statistical analysis section and Fig. 3).

Parameterization of inputs for model

Two input parameters, α and β, were estimated daily by employing a least-squares regression fitting, iterated 100 times over Eqn 8 using dendrometer measurements at 30 min intervals (Microsoft Excel 2010). To parameterize Eqn 8, piecewise linear regression (between notable break points in growth) was used to subtract the growth signal from the inner-bark measurements for all years (Zweifel & Häsler 2001; Zweifel *et al.* 2001; Mencuccini *et al.* 2013). Note that this procedure is only employed to allow estimating the coefficients of Eqn 8. Once the coefficients are obtained, Eqn 8 is then employed on the raw time series. There were days when the iteration did not converge, which may arise due to unclear diurnal patterns (e.g. high precipitation). In these cases, the non-converged values were obtained by interpolation. Each daily parameter value was calculated from midnight to the following midnight. Estimation of $\hat{\Delta}G_m$ over the course of the season was calculated from the estimated daily α and β values over the whole sampling period.

Study area

This study used meteorological, microclimate and stem measurement data collected at the University of Helsinki's Station for Measuring Forest Ecosystem-Atmosphere Relations (SMEAR II) in Hyytiälä. The station is located within the southern boreal zone in southern Finland (61°50′50″N, 24°17′41″E, 180 m a.s.l.), in an even-aged homogeneous ~50-year-old Scots pine (*Pinus sylvestris* L.) stand (Vesala *et al.* 1998). The previous stand fell in 1961, followed by prescribed burning, after which Scots pine seeds were sown. The dominant height (the average height of the 100 thickest trees per hectare) of the stand was 17.4 m and the mean stem diameter at breast height (1.3 m) was 13.0 cm. The mean annual precipitation and air temperature were 713 mm and +3.3 °C, respectively. January is typically the coldest month (mean –8.9 °C) and July the warmest (mean +15.3 °C).

Microclimate measurements

Air temperature, soil water content, photosynthetic photon flux density (PPFD), relative humidity and precipitation were continuously measured year-round, but for this study, only the periods from May 1 to October 5 in years 2007–2009 were used. Vapour pressure deficit (VPD) was calculated from the relative humidity measurements and air temperature. Relative humidity was measured with a chilled dew mirror hygrometer (M4 chilled mirror monitor; General Eastern, Woburn, MA, USA) at a height of 23 m. Air temperature was measured with platinum resistance thermometer sensors (Type PT-100; T. Pohja, Juupajoki, Finland) at a height of 8.4 m. Soil water content was measured at a depth of 17 cm using time domain reflectometry (TDR) methodology, using five unbalanced steel probes (Tektronix 1502 °C cable radar; Tektronix Inc., Redmond, WA, USA). The probe sensors were connected to a datalogger (21X; Campbell Scientific Ltd., Leics., UK) by means of multiplexers (SDMX50; Campbell Scientific Ltd.) and converted to soil water potential (Ψ_{soil}). Precipitation was collected with rain gauge AGR-100 (Environmental Measurements Ltd., Sunderland, UK). PPFD was measured above the canopy level near the tree from which the radial stem measurements were taken. The recording interval for each environmental sensor was 1 min; but for this study, the recording interval of 30 min was used.

Stem radius measurements

Radial stem variations were measured with two linear variable displacement transducers (point-dendrometers) (LVDT; model AX/5.0/S; Solartron Inc., West Sussex, UK) at a height of 15 m from one sample tree. The point-dendrometers were attached on a rectangular stainless steel frame spaced 30 mm apart and were affixed onto the stem about 20 cm below the

measuring point with screws using two attachment plates. The temperature of the frame was measured and the values were corrected to consider the combined heat expansion of the frame and wood (2×10^{-6} °C^{-1}; see Sevanto *et al.* 2005). A detailed description of the dendrometers is provided by Sevanto *et al.* (2005). The head of the first dendrometer (measuring D_x) rested on a screw that was inserted approximately 10 mm through the outer and inner bark into the superficial part of the existing xylem. This dendrometer measured changes of the xylem radius. The head of the second dendrometer (measuring D_w), measuring the whole stem radius, rested on the phloem. The phloem was exposed by incising the outer bark approximately 3 mm deep with a scalpel. Similar to microclimate measurements, the recording interval for the dendrometer measurements was 30 min.

Microcore sampling

Microcore samples were taken from four Scots pine trees within the same stand, approximately 20 m from the tree for the dendrometer measurements during the 2007–2009 growing seasons, beginning from May 1. The conditions of the microcoring site were similar to the dendrometer measurement site; hence, it is reasonable to use them as a proxy to represent stem cell growth for the trees measured with dendrometers.

In 2007, microcores were extracted with injection needles twice a week in spring and early summer and once a week in late summer. In 2008 and 2009, microcores were extracted using Trephor, a tool specifically designed for microcoring (Rossi *et al.* 2006). After the outer bark was removed, the Trephor was inserted approximately 10 mm deep into the stem at breast height (1.3 m). The microcores were dehydrated with ascending series of ethanol, cleared with Tissue-Clear (Tissue-Tek®; Sakura Finetek, Tokyo, Japan), immersed into liquid paraffin (Histowax; Leica Microsystems, Wetzlar, Germany) and embedded into paraffin blocks. Transverse radial sections were cut with a rotary microtome (Leitz 1516; Leica Microsystems). The sections were placed on microscopic slides, stained with 1% solutions of Safranin and Alcian blue, dehydrated in ascending series of ethanol and mounted into Canada balsam. Images were taken of the current-year rings with a digital CCD camera (Media Cybernetics, Inc., Bethesda, MD, USA, or MicroPublisher 3.3 RTV, QImaging, Surrey, BC, Canada). From the images, tracheid diameters were measured along one to three representative cell rows in each section with image analysis software Image-Pro Plus v. 4.1 or 7.0 (Media Cybernetics Inc.). Sampling and measurements of microcores are explained in detail in Jyske *et al.* (2014).

Statistical analysis

Intra-annual growth was divided into three phases: pre-growth, growth and post-growth. The pre-growth phase was defined as the period from May 1 to the date when the first new tracheids were observed in microcores. The growth phase was defined as the period from initial tracheid formation to the date at which 95% of seasonal radial increment was achieved, based upon dendrometer measurements. The post-growth phase was defined as the period from the end of the growth phase to October 5, when much of the season's growth has completed.

Observations on the influence of environmental factors focused on the latter two phases and were tested against the daily variation of D_w, D_b and $\hat{\Delta}G_m$. Daily variation was calculated as the difference between two consecutive daily maximum values of D_w, D_b and $\hat{\Delta}G_m$. The daily sum of precipitation and daily mean values of air temperature, VPD, Ψ_{soil} and PPFD were then compared against the daily variation using linear regression and Pearson product–moment correlation coefficient.

Finally, we compared the estimate for daily growth, denoted as g, to the estimate for the amplitude of diurnal model-derived reversible peak in $\hat{\Delta}G_m$ due to changes in osmotic concentration, P_0 (i.e. the maximum difference between the daily $\hat{\Delta}G_m$ and the linearly interpolated growth between two subsequent minima) (Fig. 3).

RESULTS

Comparison between measured and modelled radial variations and radial growth from microcores

In late March, a combination of low temperatures and considerable transpiration with limited water uptake produced a large contraction of stem radius, a situation which repeated itself each year (data not shown). The recovery of stem radius from winter contraction commenced in April for all years. Dendrometer data showed a consistent diurnal swelling and shrinking cycle beginning from weeks 20 and 21 in all years (roughly mid-May to June), with whole stem radial thickness (D_w) reaching 95% of its maximum around weeks 33 and 34 (August 13 in years 2007 and 2008, August 21 in 2009) (Fig. 4). D_w variation displayed larger diurnal amplitude than inner-bark radial thickness (D_b) variation. After mid-August, D_w shrank slightly in all study years, with a similar reduction observed for D_b. However, notably sudden, partly reversible longer-lasting patterns were observed during rainy periods. During these periods, the regular daily pattern of changes in stem radius disappeared (Fig. 5).

The seasonal accumulation of tracheids, measured from microcores, followed a pattern similar to that of stem radial variation from dendrometer data with a slight but consistent lag (Fig. 4). It is important to note that microcore measurements include only woody tissue, whereas dendrometer measurements include both woody and bark tissue. The first tracheids were formed in late May/early June (approximately June 8 in 2007, May 29 in 2008 and May 28 in 2009), with the dendrometers showing a permanent increase approximately 10 d before that. Maximum cumulative stem radius from dendrometers also occurred approximately 2 weeks earlier than the formation of the last tracheids according to the microcore measurements. In the late summer, the width of the current year ring reached levels similar to that of cumulative increment of stem radius in dendrometer data,

eventually surpassing it after mid-September. The periodic increment in consecutive measurements of microcores was compared with the corresponding periodic daily modelled growth and osmotic concentration change ($\hat{\Delta}G_m$) over the course of the season, revealing a highly significant correlation for all years ($P < 0.001$) (Fig. 6).

$\hat{\Delta}G_m$ showed overall lower cumulative radial increment than D_w and D_b. Incidentally, in 2007, $\hat{\Delta}G_m$ showed higher radial variation than D_w and D_b during the growth phase, but decreased below field-measured stem radii in late August. During periods of rain, the differences between $\hat{\Delta}G_m$, D_w and D_b decreased as the xylem water potential of the tree increased. This implicated that the proportion of reversible change to irreversible increment in D_b increased during rain. During dry periods, however, there were notable differences between $\hat{\Delta}G_m$ and measured stem radii, particularly on the diurnal scale.

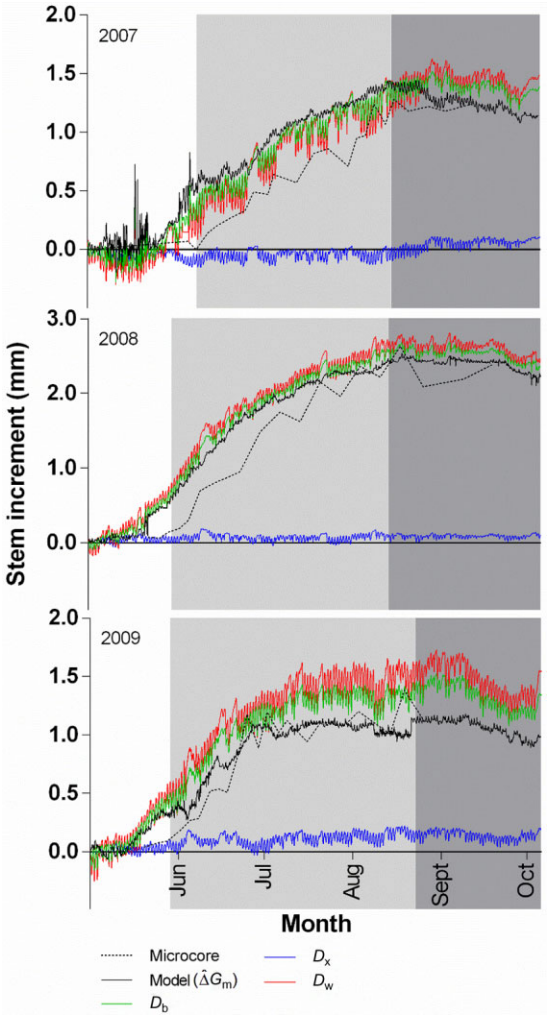

Figure 4. Seasonal course of growth from microcores, stem radius variation [whole stem (D_w), inner bark (D_b) and xylem (D_x)] and modelled growth ($\hat{\Delta}G_m$) in years 2007–2009. For each year, intra-annual growth was divided into the three phases of pre-growth (white shade), growth (light grey shade) and post-growth (dark grey shade). Point-to-point seasonal decline from microcores may be due to measuring error.

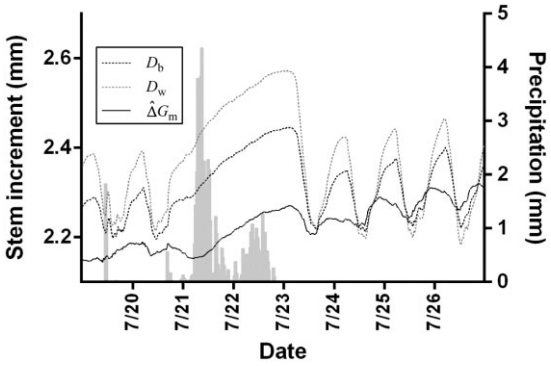

Figure 5. Daily precipitation (grey bars), measured radius variations of inner bark (D_b) and whole stem (D_w) and modelled growth increment and osmotic concentration change ($\hat{\Delta}G_m$) during the period of 19–26 July 2008. The inset graph is an enlarged view of stem variation of $\hat{\Delta}G_m$ during July 24–26. Dotted line denotes midnight. Measured and modelled radius variations were offset to 0 on May 1.

Diurnal variations of $\hat{\Delta}G_m$ revealed clearly an overall smaller amplitude than both D_b and D_w (Fig. 5). These variations began at approximately noon when the stem began to rehydrate after the lowest xylem water potential had been reached and lasted until approximately noon the following day. Daily maximum and minimum values of $\hat{\Delta}G_m$ occurred shortly before midnight and afternoon, respectively. $\hat{\Delta}G_m$ showed two distinct variations, with the first beginning in the afternoon, reaching an apex shortly before midnight and declining immediately until noon. The second, shorter variation lasts for only a few of hours around pre-dawn, declining in conjunction with the first variation. This pattern was evident in all years throughout the growing season (except during and shortly after periods of rain).

The seasonal pattern of α and β

Parameter value α showed an increasing seasonal trend in years 2007 and 2009 but a decreasing trend in 2008 (2007 trend shown in Fig. 7a) and followed daily temperature patterns exponentially (non-significant in 2007, $P < 0.05$ in 2008 and 2009) (2009 correlation shown in Fig. 7b). Mean α values of the years studied ranged from 0.40 to 0.53. The values of parameter β values were similar over the seasons during each year, with a marginal decreasing (non-significant) trend from early spring towards the end of summer. Mean β values for the three years studied varied between 1.26 and 2.30. Modelled results (dynamics of $\hat{\Delta}G_m$) were rather insensitive to α and β values (the results of a sensitivity analysis are reported in Supporting Information Appendix S1).

Effect of environmental variables on $\hat{\Delta}G_m$ and measured radial variations

The two phases (growth and post-growth) saw differences in the relationship of daily variations in D_w, D_b and $\hat{\Delta}G_m$ to environmental factors. Taking the growth and post-growth

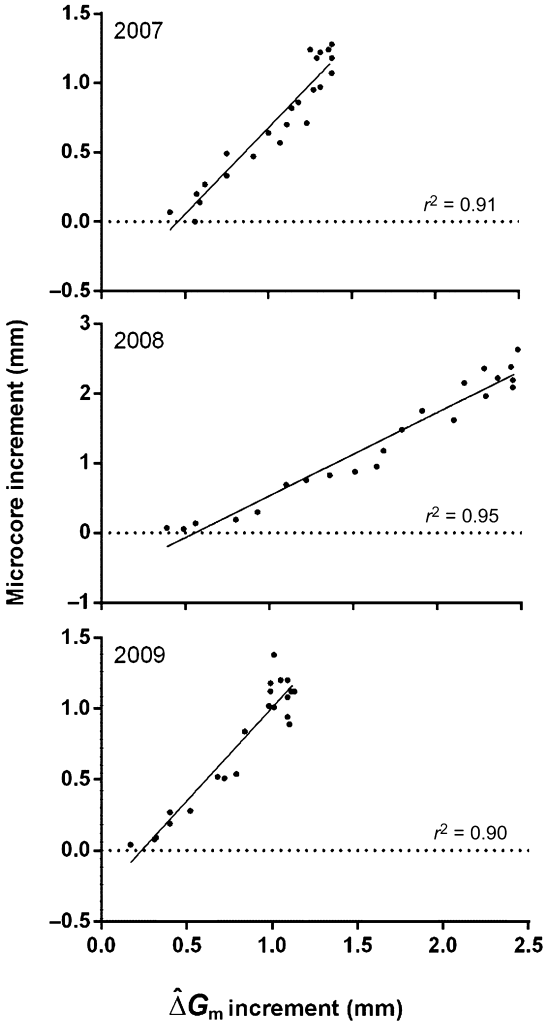

Figure 6. Regressions between the two measured consecutive radial growth increment of microcores and modelled consecutive growth for the corresponding period and osmotic concentration change ($\hat{\Delta}G_m$). Dotted lines indicate zero points. Note that sampled microcores only include woody tissue, whereas $\hat{\Delta}G_m$ includes both woody and bark tissue.

phases together, the variations of $\hat{\Delta}G_m$ were more weakly correlated to precipitation than the variations in D_w and D_b, but were more positively correlated against VPD, PPFD and temperature (Pearson's correlation analysis) (Table 2). Similarly, examining the growth and post-growth phases separately, the daily variations of D_w and D_b showed a high correlation to precipitation in all years for each phase. Variations in D_w and D_b were also highly correlated, but negatively, to PPFD during both phases in 2008 and during the growth phase only in 2007 and 2009. VPD had significant negative correlation ($P < 0.01$) with D_w and D_b in 2009 for both phases and during the post-growth phase in 2008. In the growth phase of 2008, there was a high negative correlation between the measured and modelled daily variations to Ψ_{soil} ($P < 0.01$), which was also seen during 2009's growth phase in $\hat{\Delta}G_m$. Temperature did not show significant correlations with $\hat{\Delta}G_m$ and measured stem radii in any of the years, but similarly to the VPD correlation, temperature tended to be positively correlated with $\hat{\Delta}G_m$ and negatively correlated with D_w and D_b. Finally, a significance was found for 2007 ($P < 0.01$) and 2008 ($P < 0.05$) between daily stem variation of $\hat{\Delta}G_m$ and temperature (Fig. 8).

Linkage between growth and osmotic concentration

The connection between the estimated daily increment of $\hat{\Delta}G_m$, g (derived from $\hat{\Delta}G_m$) and the daily amplitude in $\hat{\Delta}G_m$ (denoted as P_0, and representing the change of osmotic concentration; cf. Fig. 3) was further analysed. There was a close correlation between these variables in all years, and the regression lines were practically the same for each year (Fig. 9). The reversible osmotic-driven daily amplitude of $\hat{\Delta}G_m$ was maximally 0.03 mm. This was consistent from year-to-year, whereas g daily increment varied from –0.05 to 0.1 mm. If the reversible amplitude was less than ~0.005 mm, then the inner bark actually shrank at the most, roughly 0.05 mm. When P_0 was high, daily variation was high. This relationship was quite robust from year-to-year, explaining approximately 70–75% of growth. This correlation was much higher than that of $\hat{\Delta}G_m$ alone with PPFD or temperature. The daily amplitude of P_0 was also positive and significantly correlated with PPFD and temperature during rainless days ($P < 0.01$) (Fig. 10).

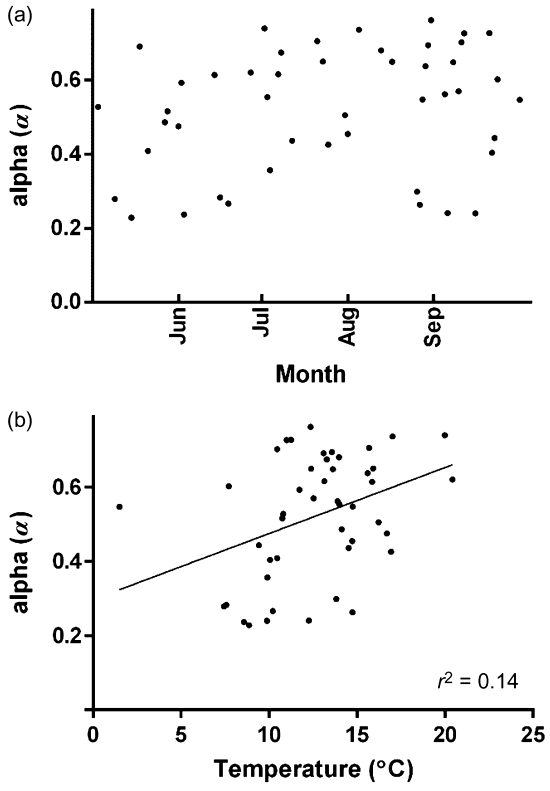

Figure 7. (a) Seasonal course of radial hydraulic conductance between the xylem and inner-bark (α) and (b) regression between radial hydraulic conductance and temperature in 2009.

Table 2. Pearson's correlation coefficients between environmental factors, measured stem radial variations (whole stem and inner bark) and $\hat{\Delta}G_m$ from 2007 to 2009, separated into growth, post-growth and the combined growth and post-growth phases

	Growth phase			Post-growth phase			Year (growth and post-growth phases)		
Parameter	2007	2008	2009	2007	2008	2009	2007	2008	2009
Precipitation									
D_w	0.333**	0.455**	0.502**	0.416**	0.368**	0.465**	0.362**	0.424**	0.496**
D_b	0.338**	0.430**	0.425**	0.444**	0.312*	0.477**	0.371**	0.386**	0.434**
$\hat{\Delta}G_m$	0.060	0.030	–0.194	0.140	0.075	0.080	0.111	0.070	–0.124
PPFD									
D_w	–0.331**	–0.341**	–0.336**	–0.053	–0.335*	–0.245	–0.087	–0.026	–0.157
D_b	–0.261*	–0.307**	–0.238*	–0.143	–0.349**	–0.279	–0.047	0.040	–0.080
$\hat{\Delta}G_m$	0.178	–0.223	0.161	–0.202	–0.115	0.107	0.214*	0.132	0.195*
Temperature									
D_w	–0.137	–0.089	–0.218*	0.005	–0.051	–0.108	0.076	0.145	–0.102
D_b	–0.038	0.021	–0.182	0.065	0.041	–0.013	0.161	0.263**	–0.039
$\hat{\Delta}G_m$	0.323*	–0.024	0.042	0.218	0.129	0.208	0.404**	0.277**	0.140
VPD									
D_w	–0.222	–0.131	–0.323**	–0.166	–0.491**	–0.401**	–0.082	0.029	–0.211*
D_b	–0.136	–0.032	–0.244*	–0.181	–0.494**	–0.408**	–0.007	0.128	–0.138
$\hat{\Delta}G_m$	0.286*	–0.022	0.136	–0.071	–0.130	0.087	0.310**	0.170	0.168
Ψ_{soil}									
D_w	–0.032	–0.317**	0.100	–0.032	0.063	0.228	–0.074	–0.408**	0.167
D_b	–0.055	–0.376**	0.211	–0.047	0.088	0.265	–0.097	–0.482**	0.260**
$\hat{\Delta}G_m$	–0.091	–0.325**	0.445**	0.091	0.082	0.252	–0.084	–0.426**	0.397**

*$P < 0.05$; **$P < 0.01$.
PPFD, photosynthetic photon flux density; VPD, vapour pressure deficit.

DISCUSSION

Comparison of model results to measured dendrometer variations and growth from microcores

In this study, a simple hydraulic model, based upon the principles of Hooke's law, was used to separate water-induced changes of the xylem from those of inner-tissue radius measured with dendrometers. Separating this predominantly daily radial change reveals a proxy for radial growth and changes due to osmotic concentration ($\hat{\Delta}G_m$).

Similar to direct dendrometer measurements, modelled periodic $\hat{\Delta}G_m$ compared rather well with measured periodic xylem increment derived from the sampled microcores. The regression of microcore measurements to corresponding variations of $\hat{\Delta}G_m$ over the same period showed consistently high year-to-year correlations (Fig. 6). The microcore-derived increment was consistently smaller than that of $\hat{\Delta}G_m$, which was expected, as the former does not include phloem growth, whereas the latter does. Whole stem (D_w) and inner-bark (D_b) radial variations could also be used cautiously in non-water-stressed environments for assessing growth over longer time periods, despite the fact that these variations also include sizable water-driven changes (Klepper *et al*. 1971). This is understandable as there are no large seasonal net changes in the xylem water status. At shorter timescales, however (i.e. daily and weekly timescale), the use of direct dendrometer data to assess growth is problematic, as radial growth is small compared with the daily radial changes due to xylem water status. This is reflected by how different environmental variables are correlated to growth (Table 2).

When using dendrometer measurements directly, daily stem variation was mainly related to variables linked to tree hydraulics. As previous studies have shown, either measured xylem (Irvine & Grace 1997; Perämäki *et al*. 2001) or whole stem (Offenthaler *et al*. 2001; Zweifel & Häsler 2001; Zweifel *et al*. 2001) radial changes are approximately linearly proportional to changes in stem water potential. Here, the dendrometer measurements had the highest (positive) correlation to precipitation, followed by a high but negative correlation to PPFD. High negative correlation to PPFD was expected, as it correlates with high transpiration and low leaf water potentials. In addition, low PPFD is generally associated with heavy cloud cover and days with high precipitation (Wright & Van Schaik 1994). After removing the water-induced changes, $\hat{\Delta}G_m$ was mainly and positively correlated with temperature and PPFD, both of which are directly linked with metabolic activity and tree productivity (Table 2, Fig. 8).

The patterns of tracheid accumulation showed delayed initiation and cessation of woody tissue of approximately 10–14 d compared with $\hat{\Delta}G_m$. These patterns follow closely the microcore observations from Mäkinen *et al*. (2008), where similar delays were found to be at a minimum of 2 weeks relative to dendrometer data. One reason for the difference is that microcore measurements do not include phloem growth as $\hat{\Delta}G_m$ derived values do. It has been

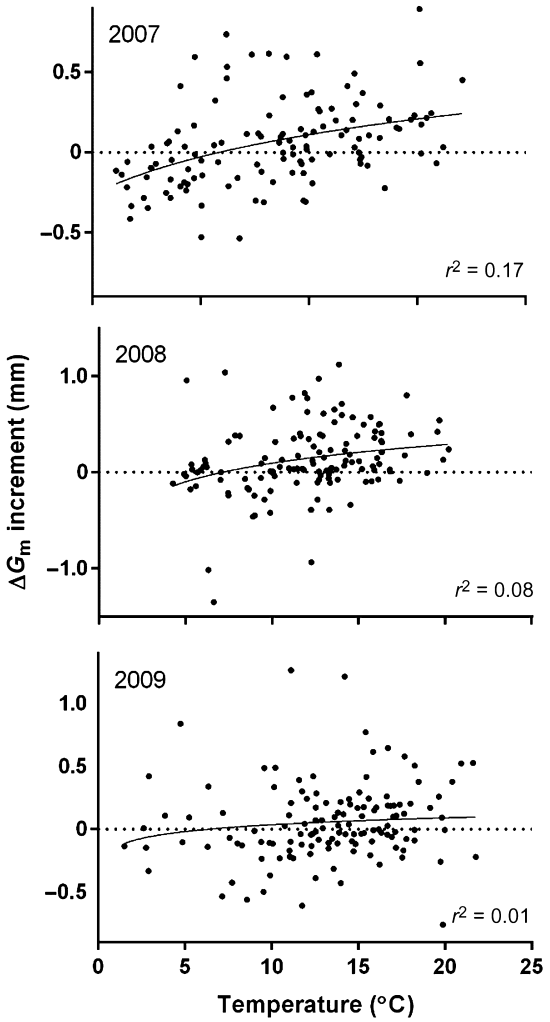

Figure 8. The relationship between daily stem variation of $\hat{\Delta}G_m$ and daily mean temperature of combined growth and post-growth phases. A high significant relationship was found in 2007 and 2008 ($P < 0.01$).

observed that the bark growth in Scots pine starts 10–20 d prior to the xylem growth (Antonova & Stasova 2006), which is consistent with our observations of growth initiation. Delays could also be caused by the microcore measuring technique, as compression of newly developed cells may occur. These delays were observed during the growth phase but largely disappeared towards the end of the post-growth phase when growth in the cambium ceased. Moreover, $\hat{\Delta}G_m$ derived values were always larger than those from microcore, which is consistent due to the latter not including phloem growth and compression of non-lignified cells when sampling.

Linkage between daily growth and osmotic concentration in the model results

We found a high correlation between the daily amplitude of osmotic concentrations (P_0) and estimated daily modelled growth (g) (Fig. 9). P_0 could further be expressed in units of osmotic pressure using Eqn 2 by substituting osmotic pressure for ΔP_b, provided that the elastic modulus of the inner bark is known (we do not attempt this here). As Mencuccini *et al*. (2013) and De Swaef *et al*. (2013) identified, the osmotic changes of the inner bark can be related to phloem transport. Such a relationship can be expected, as growth depends upon available sugars, which are the substance needed for cell wall formation. Sugars are also osmolytes, which provide turgor pressure for cell wall expansion (Hölttä *et al*. 2010; Pantin *et al*. 2012). When P_0 was small, we observed that inner-bark tissue shrank. The maximal shrinkage was ~0.05 mm, suggesting the magnitude of turgor changes on bark dimensions. A similar order of magnitude in correlation was also seen between the modelled growth and the microcore results in 2007 and 2008 (Fig. 4). In addition, the data revealed that the daily osmotic change was linked to PPFD and temperature (Fig. 10). However, the correlations were not very high, but still higher than for the modelled daily growth against the

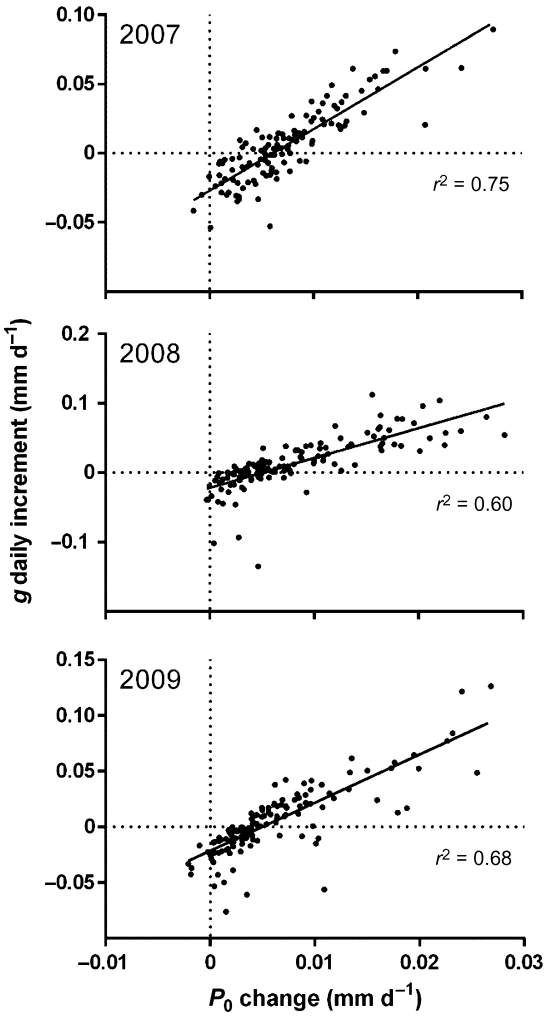

Figure 9. Regression between estimated g daily increment and osmotic concentration (P_0) in from 2007 to 2009 during the growth and post-growth phase. As daily growth change is estimated from $\hat{\Delta}G_m$, it also includes changes due to osmotic concentration, which may cause negative values. Dotted lines indicate zero points.

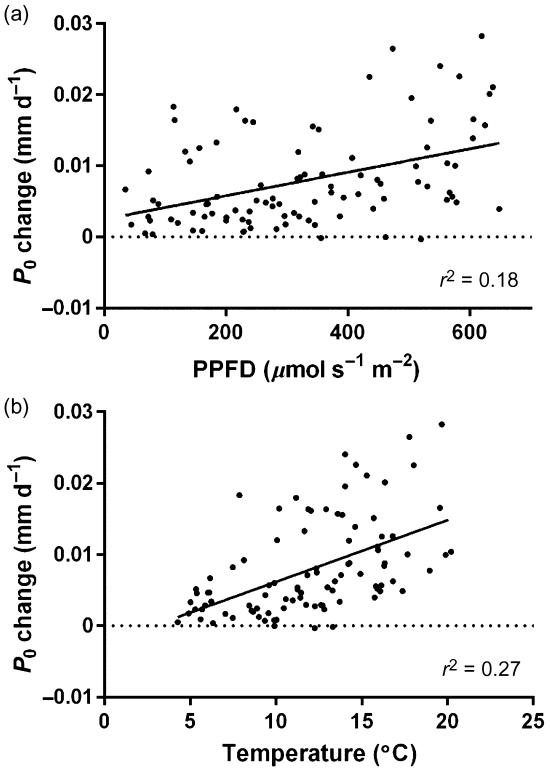

Figure 10. Correlation of the estimated daily amplitude in osmotic pressure (P_0) to (a) daily average photosynthetic photon flux density (PPFD) and (b) to temperature. In both cases, P_0 was found to be significantly correlated with these two variables ($P < 0.01$). Rain days were not included in the calculation. Dotted lines indicate the level of zero osmotic pressure.

environmental variables. For example, temperature alone accounted for less than 20% of daily growth, which is much less than the correlation with the osmotic change. This however was expected as changes in osmotic concentration are inexplicably linked with phloem transport, as supported by observations from Mencuccini *et al.* (2013).

Diurnal and seasonal variations of $\hat{\Delta}G_m$

During a day, $\hat{\Delta}G_m$ typically exhibited two distinct periods of change due to osmotic concentration movement. The first change occurred around noon, when the stem swelled rapidly until the evening, and shrinking occurred until late morning of the following day (Fig. 5, inset). The swelling during this period suggested an osmotic concentration movement along the stem, which could be attributed to the start of photosynthesis and the rapid propagation of osmotic concentration along the phloem. The second change occurred during the first change's shrinking stage, approximately around predawn and lasting only a few hours. This second swelling could be caused by axial pressure propagation in the phloem, induced by the first swelling period. As a result, shoot turgor pressure may have increased if the first swelling was caused by photosynthesis and resulted in sugar accumulation in the shoot (Moore 1995). This turgor pushes a pressure pulse down along the phloem to initiate photosynthate allocation. As the pulse travels faster than the sugar flow in the phloem, the short increase in $\hat{\Delta}G_m$ during this period may be due to this phenomenon. Similar diurnal changes in Scots pine were reported by Mencuccini *et al.* (2013) and have been observed in other studies with *Lupinus albus* L. (Sharkey & Pate 1976), *Nicotiana glauca* Grah. (Hocking 1980) and *Prunus persica* (L.) Batsch (Fishman & Génard 1998), and predicted in modelling studies (Hölttä *et al.* 2006). Their findings confirmed that sugar pools are accumulated during the day and translocated during the night. A study on *Abies balsamea* showed that stem growth continues constantly throughout the day (Deslauriers *et al.* 2003). However, according to the model proposed, growth occurred mainly during the night, when transpiration has ceased and water tension has relaxed. Similar findings have been reported in studies on sap flow dynamics (Daudet *et al.* 2005; Steppe *et al.* 2006; De Schepper & Steppe 2010; Hölttä *et al.* 2010). During the night, $\hat{\Delta}G_m$ is dependent upon temperature, whereas water potential is fairly constant and less negative than daytime values. Therefore, many authors have suggested that nighttime conditions are more important for growth than daytime conditions (Antonova & Stasova 1993; Antonova *et al.* 1995; Berman & Dejong 1997; Luxmoore *et al.* 1998; Zweifel & Häsler 2001; Zweifel *et al.* 2001; Zhai *et al.* 2012).

Seasonal growth was separated into growth and post-growth phases for all years, and $\hat{\Delta}G_m$, D_w and D_b were further analysed by comparing their respective daily stem variations to environmental factors. Generally, the growth phase saw an increase of measured and modelled cumulative radial increment, which ended approximately at the beginning of the post-growth phase. During this phase, temperature was the most limiting factor for growth (Table 2), especially when combining both growth and post-growth phases. Daily mean temperature during these two phases was significantly correlated with daily $\hat{\Delta}G_m$ variation in 2007 and 2008 ($P < 0.01$). A study from Zweifel *et al.* (2005) demonstrated that radial variation is largely affected by Ψ_{soil} if the soil is dry, and by VPD when root water availability is high. This could be seen during 2009's growth phase, when $\hat{\Delta}G_m$ showed a high value of the Pearson coefficient with Ψ_{soil} while a non-significant correlation with VPD. This sharply contrasts 2007's growth phase, when the variation of $\hat{\Delta}G_m$ was significantly affected by VPD but not with Ψ_{soil}; and also observed when both growth and post-growth phases were combined.

In comparison to the growth phase, daily variations during the post-growth phase were considerably lower because cessation of tree growth and the onset of tree dormancy and winter hardiness processes have begun. However, growth processes still persist – albeit at a lower rate than during the growth phase. Changes to stem radius were mainly related to temperature and water availability. Growth in this phase was more dependent on temperature than on precipitation and PPFD. This is similar to a previous study, where the temperature's contribution to overall growth was greater than precipitation, but high soil water content was still essential for tree function and growth (Antonova & Stasova 1993). Days

with precipitation affected slightly $\hat{\Delta}G_m$ dynamics (Fig. 5). This can be seen especially in 2007 and 2009, which showed greater growth due to precipitation, compared with their respective year's growth phase (Table 2). As water availability is scarcer during this phase than during the growth phase, it follows that growth sensitivity to precipitation increases. During these rainy days, it could be suggested that growth processes are elevated. However, it is important to note that isolating growth due to changes solely of temperature or precipitation is difficult. Moehring & Ralston (1967) and Antonova & Stasova (1997) have reported temperature and precipitation having varying influences on growth at different stages of wood formation, but caution is needed when interpreting these type of results, as direct dendrometer measurements overemphasize the influence of growth due to precipitation. Furthermore, a study from Zhai *et al*. (2012) indicated that when precipitation had a positive effect on growth, the temperature's impact on growth was less than that of tree water status. However, the requirements for both early and late wood formation (during the post-growth phase) have varying temperature and water availability requirements. Early wood formation demands high water availability with a general daily mean temperature of 21 °C, whereas late wood development occurs after a period of water stress (due to reduced Ψ_{soil}). For the latter, initiation of stem growth could potentially occur again in the late summer if soil water is replenished and temperature returns to optimum levels. This re-initiation may have occurred in 2008, as high Ψ_{soil} (and subsequently high water availability) resulted in $\hat{\Delta}G_m$ levels similar to that of its growth phase. This could suggest that growth in 2008 was contingent more upon temperature than precipitation (Table 2). This contrasted observations from 2007, where low Ψ_{soil} was observed. This implied that the driving factor for growth required higher precipitation and lower VPD. In each year, though, the daily growth was most strongly correlated with the daily osmotic changes.

Potential improvements to the model

Estimation of $\hat{\Delta}G_m$ could be expanded by better exploring the water dynamics between xylem and inner bark. For example, this study used a constant α and β over the measurement period, but a model reflecting actual daily variations of α and β could potentially yield a better estimation. Parameter α could be affected at least by the aquaporin activity and by temperature through its effect on viscosity (Steppe *et al*. 2012; Mencuccini *et al*. 2013). Rainy days imposed a modelling challenge and erratic signals resulted even after the removal of hydraulic influences. For example, the model does not consider the possible infiltration of external moisture from stem surface into bark tissue (Katz *et al*. 1989). However, the exclusion of rainy days did not significantly affect $\hat{\Delta}G_m$ dynamics.

CONCLUSION

Current methods to quantify measured stem variations using band, one-point (measuring whole stem) or two-point (measuring xylem and whole stem) dendrometers include both water-induced changes and growth. With these devices, it is very difficult to separate growth from measured stem radial variation – particularly at short timescales. We used a simple hydraulic model to separate the water-induced signal in the inner-bark radius to reveal a proxy signal caused by cambial growth and osmotic concentration change. This signal gave a clear interpretation of how growth and osmotic concentration dynamic function from a diurnal to seasonal scale. As a major new step, the analysis allowed for comparison of cambial growth and osmotic concentration change against environmental variables. These comparisons would normally be masked by water-potential induced changes. The approach could thus be useful in assessing how these factors affect also other physiological processes of the tree. The model also brings us closer to developing a method of quantifying osmotic-related stem radial changes, which could be used to interpret sugar loading and unloading within the phloem. Finally, radial hydraulic conductance and stem tissue elasticity were not only employed as model inputs, but their analysis allowed us to explore the significance of their temporal dynamics in tree–water relations.

ACKNOWLEDGMENTS

This paper was supported by the Academy of Finland (Project Nos. 140781 and 268342), Finnish Centre of Excellence (Grant Nos. 1118615, 257641 and 265504), MultiTree Project 257641, EcoGrad 265504, and was conducted in the framework of the COST action, STReESS (FP1106).

REFERENCES

Altman A. & Goren R. (1974) Growth and dormancy cycles in citrus bud cultures and their hormonal control. *Physiologia Plantarum* **30,** 240–245.

Antonova G. & Stasova V. (2006) Seasonal development of phloem in Scots pine stems. *Russian Journal of Developmental Biology* **37,** 306–320.

Antonova G.F. & Stasova V.V. (1993) Effects of environmental factors on wood formation in Scots pine stems. *Trees* **7,** 214–219.

Antonova G.F. & Stasova V.V. (1997) Effects of environmental factors on wood formation in larch (*Larix sibirica* Ldb.) stems. *Trees* **11,** 462–468.

Antonova G.F., Cherkashin V.P., Stasova V.V. & Varaksina T.N. (1995) Daily dynamics in xylem cell radial growth of Scots pine (*Pinus sylvestris* L.). *Trees* **10,** 24–30.

Berman M.E. & Dejong T.M. (1997) Diurnal patterns of stem extension growth in peach (*Prunus persica*): temperature and fluctuations in water status determine growth rate. *Physiologia Plantarum* **100,** 361–370.

Bordiert R. (1994) Water status and development of tropical trees during seasonal drought. *Trees* **8,** 115–125.

Buell M.F., Buell H.F., Small J.A. & Monk C.D. (1961) Drought effect on radial growth of trees in the William L. Hutcheson memorial forest. *Bulletin of the Torrey Botanical Club* **88,** 176–180.

Daudet F.-A., Améglio T., Cochard H., Archilla O. & Lacointe A. (2005) Experimental analysis of the role of water and carbon in tree stem diameter variations. *Journal of Experimental Botany* **56,** 135–144.

De Schepper V. & Steppe K. (2010) Development and verification of a water and sugar transport model using measured stem diameter variations. *Journal of Experimental Botany* **61,** 2083–2099.

De Swaef T., Driever S.M., Van Meulebroek L., Vanhaecke L., Marcelis L.F.M. & Steppe K. (2013) Understanding the effect of carbon status on stem diameter variations. *Annals of Botany* **111,** 31–46.

Deslauriers A. & Morin H. (2005) Intra-annual tracheid production in balsam fir stems and the effect of meteorological variables. *Trees* **19,** 402–408.

Deslauriers A., Morin H., Urbinati C. & Carrer M. (2003) Daily weather response of balsam fir (*Abies balsamea* (L.) Mill.) stem radius increment from dendrometer analysis in the boreal forests of Quebec (Canada). *Trees* **17,** 477–484.

Fishman S. & Génard M. (1998) A biophysical model of fruit growth: simulation of seasonal and diurnal dynamics of mass. *Plant, Cell & Environment* **21,** 739–752.

Gall R., Landolt W., Schleppi P., Michellod V. & Bucher J. (2002) Water content and bark thickness of Norway spruce (*Picea abies*) stems: phloem water capacitance and xylem sap flow. *Tree Physiology* **22,** 613–623.

Hocking P.J. (1980) The composition of phloem exudate and xylem sap from tree tobacco (*Nicotiana glauca* Grah). *Annals of Botany* **45,** 633–643.

Hölttä T., Vesala T., Sevanto S., Perämäki M. & Nikinmaa E. (2006) Modeling xylem and phloem water flows in trees according to cohesion theory and Münch hypothesis. *Trees* **20,** 67–78.

Hölttä T., Mencuccini M. & Nikinmaa E. (2009) Linking phloem function to structure: analysis with a coupled xylem–phloem transport model. *Journal of Theoretical Biology* **259,** 325–337.

Hölttä T., Mäkinen H., Nöjd P., Mäkelä A. & Nikinmaa E. (2010) A physiological model of softwood cambial growth. *Tree Physiology* **30,** 1235–1252.

Irvine J. & Grace J. (1997) Continuous measurements of water tensions in the xylem of trees based on the elastic properties of wood. *Planta* **202,** 455–461.

Jyske T., Mäkinen H., Kalliokoski T. & Nöjd P. (2014) Intra-annual tracheid production of Norway spruce and Scots pine across a latitudinal gradient in Finland. *Agricultural and Forest Meteorology* **194,** 241–254.

Katz C., Oren R., Schulze E.-D. & Milburn J. (1989) Uptake of water and solutes through twigs of *Picea abies* (L.) Karst. *Trees* **3,** 33–37.

Klepper B., Browning V.D. & Taylor H.M. (1971) Stem diameter in relation to plant water status. *Plant Physiology* **48,** 683–685.

Luxmoore R.J., Hanson P.J., Beauchamp J.J. & Joslin J.D. (1998) Passive nighttime warming facility for forest ecosystem research. *Tree Physiology* **18,** 615–623.

Mäkinen H., Seo J.-W., Nöjd P., Schmitt U. & Jalkanen R. (2008) Seasonal dynamics of wood formation: a comparison between pinning, microcoring and dendrometer measurements. *European Journal of Forest Research* **127,** 235–245.

Mencuccini M., Hölttä T., Sevanto S. & Nikinmaa E. (2013) Concurrent measurements of change in the bark and xylem diameters of trees reveal a phloem-generated turgor signal. *New Phytologist* **198,** 1143–1154.

Moehring D.M. & Ralston C.W. (1967) Diameter growth of loblolly pine related to available soil moisture and rate of soil moisture loss. *Soil Science Society of America Journal* **31,** 560–562.

Moore P. (1995) Temporal and spatial regulation of sucrose accumulation in the sugarcane stem. *Functional Plant Biology* **22,** 661–679.

Offenthaler I., Hietz P. & Richter H. (2001) Wood diameter indicates diurnal and long-term patterns of xylem water potential in Norway spruce. *Trees* **15,** 215–221.

Pantin F., Simonneau T. & Muller B. (2012) Coming of leaf age: control of growth by hydraulics and metabolics during leaf ontogeny. *New Phytologist* **196,** 349–366.

Perämäki M., Nikinmaa E., Sevanto S., Ilvesniemi H., Siivola E., Hari P. & Vesala T. (2001) Tree stem diameter variations and transpiration in Scots pine: an analysis using a dynamic sap flow model. *Tree Physiology* **21,** 889–897.

Rossi S., Anfodillo T. & Menardi R. (2006) Trephor: a new tool for sampling microcores from tree stems. *IAWA Journal* **27,** 89–97.

Sevanto S., Vesala T., Perämäki M. & Nikinmaa E. (2003) Sugar transport together with environmental conditions controls time lags between xylem and stem diameter changes. *Plant, Cell & Environment* **26,** 1257–1265.

Sevanto S., Hölttä T., Hirsikko A., Vesala T. & Nikinmaa E. (2005) Determination of thermal expansion of green wood and the accuracy of tree stem diameter variation measurements. *Boreal Environment Research* **10,** 437–445.

Sevanto S., Hölttä T., Markkanen T., Perämäki M., Nikinmaa E. & Vesala T. (2005) Relationships between diurnal xylem diameter variation and environmental factors in Scots pine. *Boreal Environment Research* **10,** 447–458.

Sevanto S., Hölttä T. & Holbrook N.M. (2011) Effects of the hydraulic coupling between xylem and phloem on diurnal phloem diameter variation. *Plant, Cell & Environment* **34,** 690–703.

Sharkey P.J. & Pate J.S. (1976) Translocation from leaves to fruits of a legume, studied by a phloem bleeding technique: diurnal changes and effects of continuous darkness. *Planta* **128,** 63–72.

Steppe K., De Pauw D.J.W., Lemeur R. & Vanrolleghem P.A. (2006) A mathematical model linking tree sap flow dynamics to daily stem diameter fluctuations and radial stem growth. *Tree Physiology* **26,** 257–273.

Steppe K., Cochard H., Lacointe A. & Améglio T. (2012) Could rapid diameter changes be facilitated by a variable hydraulic conductance? *Plant, Cell & Environment* **35,** 150–157.

Vesala T., Haataja J., Aalto P., Altimir N., Buzorius G., Garam E., . . . Keronen P. (1998) Long-term field measurements of atmosphere-surface interactions in boreal forest combining forest ecology, micrometeorology, aerosol physics and atmospheric chemistry. *Trends in Heat, Mass and Momentum Transfer* **4,** 17–35.

Whitehead D. & Jarvis P.G. (1981) Coniferous forests and plantations. In *Water Deficits and Plant Growth* (ed. T.T. Kozlowski), pp. 90–119. Academic Press, New York, NY, USA.

Wright S.J. & Van Schaik C.P. (1994) Light and the phenology of tropical trees. *American Naturalist* **143,** 192–199.

Zhai L., Bergeron Y., Huang J.G. & Berninger F. (2012) Variation in intra-annual wood formation, and foliage and shoot development of three major Canadian boreal tree species. *American Journal of Botany* **99,** 827–837.

Zweifel R. & Häsler R. (2001) Dynamics of water storage in mature subalpine *Picea abies*: temporal and spatial patterns of change in stem radius. *Tree Physiology* **21,** 561–569.

Zweifel R., Item H. & Häsler R. (2001) Link between diurnal stem radius changes and tree water relations. *Tree Physiology* **21,** 869–877.

Zweifel R., Zimmermann L. & Newbery D.M. (2005) Modeling tree water deficit from microclimate: an approach to quantifying drought stress. *Tree Physiology* **25,** 147–156.

Received 7 November 2014; received in revised form 22 February 2015; accepted for publication 5 March 2015

SUPPORTING INFORMATION

Additional Supporting Information may be found in the online version of this article at the publisher's web-site:

Appendix S1. Sensitivity analysis.